Preprints of the 21st IFAC World Congress (Virtual)
Berlin, Germany, July 12-17, 2020

A comparison of low-complexity charging and balancing protocols with degradation awareness for a string of Li-ion cells

Alejandro Goldar Michel Kinnaert Emanuele Garone

SAAS, Université libre de Bruxelles, Brussels, Belgium
(e-mail: agoldard, michel.kinnaert, egarone@ulb.ac.be).

Abstract This work introduces and compares low-computational cost MPC-based algorithms based on a reduced-order electrochemical model, the Equivalent Hydraulic Model (EHM), for the fast charge and balance of a string of battery cells accounting for degradation-related phenomena. The balance is carried out through a fully shunting grid. The shunting scenarios are described in two different approaches, namely: binary variables and pulse with modulation (PWM). Due to the complexity of solving nonlinear and non-convex constrained optimal problems, we approximate the balancing grid configurations of the string as subsystems to solve an optimization problem that follows the maximization over current and configuration of the string, while minimizing the charging current of each subsystem. Numerical results show that a PWM-based approach outperforms a mixed-integer approach, showing a charging time three times lower.

Keywords: Li-ion battery packs, fast charge and balance, degradation awareness, equivalent hydraulic model (EHM), model predictive control (MPC)

1. INTRODUCTION

A battery pack is a series-parallel arrangement of Li-ion cells built to fulfill power and capacity demands. Theoretically, all the cells in the pack have identical characteristics; thus their performance should be alike given any charging current profile. However, cells might not react in the same way during the charge, showing operational imbalances that might come from manufacturing differences, localized temperature changes across the pack, and different evolving degradation rates (Quinn and Hartley, 2013).

Current commercial balancing protocols equalize voltage imbalances, within the pack, through dissipation of the excess energy (passive balancing) or the re-distribution of this energy (active balancing) from the over-charged cells to the non-charged ones. Most of the current balancing schemes depend on *ad-hoc* pre-defined balancing grids that may include one or several resistors (in passive balancing) or different types of transferring devices (in active balancing).

The main criterion to choose between passive or active balancing underlies on the implementation cost and the balancing time, i.e., the time needed to transfer energy from one cell to another. Although widely implemented due to low implementation costs, passive balancing significantly wastes the energy and may increase the temperature of the pack (Cao et al., 2008). Instead, active balancing re-distributes the excess of energy in one cell to another (cell-to-cell approach) or to the battery pack (cell-to-pack approach). The re-distribution of energy requires a longer balancing period than the dissipation. Theoretically, the lowest active balancing time for a pack of N-cells can be achieved with $N-1$ transferring devices, and $N(N-1)/2$ connections between cells (Quinn and Hartley, 2013), whose implementation cost might be prohibitively high for battery packs with a large number of cells.

Due to the wide range of balancing devices, and the different battery pack configurations, literature mainly focuses on comparing balancing strategies given a battery pack topology (Cao et al., 2008; Gallardo-Lozano et al., 2014). As the configurations effects the equalization protocol, the literature as well focuses on comparing the performance of balancing grids in cell-to-pack and cell-to-cell configurations (Preindl et al., 2013), and the impact of the topologies between transferring devices and cells (Quinn and Hartley, 2013)). Although a vast amount of contributions on balancing grids can be found in the literature, many of them are logic-based strategies that equalize the cells accounting for voltage imbalances without taking explicitly into account suitable models able to describe the electrochemical phenomena inside of each cell nor the effects of a varying charging current. The balance is assumed to be done during an idle time of the charge, where the current passing through the pack is fixed and constant.

To suitably equalize the cells within the pack, while decreasing the balancing time, some contributions have developed policies within the framework of model predictive control (MPC). In this sense, Altaf et al. (2016) introduce an equalizing MPC-based strategy for the discharge of the pack to maintain a given load, while avoiding voltage

⋆ This work is performed within the framework of the BATWAL project (Convention 1318146, PE PlanMarshall 2.vert) financed by the Walloon region.

relaxations in the equalization. Instead of using voltage imbalances, Samadi and Saif (2014) propose a nonlinear MPC policy, solved using genetic algorithms, to equalize SOC imbalances in two serially connected batteries by switching the modes of a DC-DC converter. McCurlie et al. (2016) introduce an MPC-based technique to reduce the balancing time in a cell-to-pack/pack-to-cell configuration. Preindl (2017) addresses the interaction between an MPC-based re-distributive charging and balancing strategy with an auxiliary power module, comparing the performance in a centralized policy (charging and balancing in a policy) and in a distributed scheme.

Although optimal balancing strategies have been developed, the fast charging and balancing problem accounting for the electrochemical degradation phenomena inside of the cells has not been totally addressed. Quite recently, Pozzi et al. (2019) has introduced a nonlinear constrained policy for the fast charge and balance of a string of Li-ion cells accounting for degradation limits. This strategy resorts to a complete shunting of the energy in each cell by suitably manipulating switches. Therefore, an overcharged or risky battery is by-passed to avoid further damage. To avoid the complexity of a mixed-integer nonlinear optimization problem, Pozzi et al. (2019) consider a pulse-width modulation (PWM) approach for the performance of the switches connected to each cell. Using the PWM approach, both the duty cycle of each switch and the string charging current are obtained by solving an optimal constrained problem. Although outperforming commercial balancing, the resulting nonlinear MPC-based policy might be time consuming in cheap battery management systems (BMSs), and challenging to solve at fast sampling rates.

The goal of this work is to develop algorithms "light" enough to be implemented in BMSs to charge and balance (full shunting) the pack in the shortest time possible, while accounting for the limits that may accelerate the aging of each cell (plating in the anode and solvent oxidation in the cathode). Despite the complexity of the resulting MPC-based charging/balancing policies, we propose two sub-optimal algorithms, addressing the shunting grid by two different approaches: i) an integer (binary) approach and ii) pulse-width modulation.

2. DESCRIPTION OF THE MODEL AND THE DEGRADATION-AWARE CONSTRAINTS

To develop "light" algorithms to charge and balance faster a battery pack, we require a model able to capture the main electrochemical phenomena and the main degradation mechanisms in each cell within the battery, while providing the lowest computational burden possible.

In the case of single cells, several kinds of models have been used to characterize cell dynamics within charging policies, ranging from RC-like models (equivalent circuit models, ECMs) that characterize well the macroscopic electrical performance of the cell (Hu et al., 2015), to electrochemical models (EChMs) based on PDEs that capture the inner electrochemical states of the cell (Perez et al., 2017). Although EChMs provide a reliable framework to characterize cell electrochemical dynamics, they are based on partial differential equations and algebraic relations that add computational complexity to the charging policy. Within the constrained control framework (Romagnoli et al., 2019), a linear model derived from full-order EChMs, called the equivalent hydraulic model (EHM), has shown strong evidence of a good trade-off between electrochemical meaning and computational complexity. (Romagnoli et al., 2019),

2.1 The Equivalent Hydraulic Model

The Equivalent Hydraulic Model (EHM) (Milocco et al., 2014) is an ODE model with linear dynamics and nonlinear output, which describes the main electrochemical phenomena occurring inside the battery in terms of two electrochemical states, namely: the state of charge (SOC) and the critical surface concentration (CSC), which represent Li-ion concentrations in each of the cell electrodes.

During the charge of a cell, the current passing through it generates overpotentials in the positive electrode (cathode) and in the negative electrode (anode). The difference between both overpotentials oxidizes lithium in the cathode generating Li-ions, which travel to the anode, depositing themselves within its carbon matrix. This lithium transportation phenomenon in each cell electrode (seen as a single particle, Fig.1(a)) is characterized by the EHM in terms of hydraulic relations between the levels of two tanks (q_1 and q_2 (Fig. 1(b)) that represent the lithium concentrations in the core (χ fraction) and on the surface (1-χ fraction) of the electrode, respectively. Thus the state of charge (SOC) represents the average concentration in the core and in the surface of the electrode (i.e. $\text{SOC} = (1-\chi)q_1 + \chi q_2$), and the critical surface concentration (CSC) represents the average concentration only on the surface of the electrode (i.e., $\text{CSC} = q_1$).

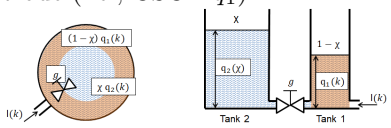

(a) Electrode (b) EHM

Figure 1. Hydraulic analogy of the EHM.

Although the EHM states describe transportation phenomena in both electrodes, the diffusion dynamics of the cathode are typically much faster than the dynamics of the anode, thus a linear relation between the cathode and the anode can be assumed as

$$\text{SOC}^+(k) = \rho \text{SOC}(k) + \sigma \tag{1a}$$
$$\text{CSC}^+(k) = \text{SOC}^+(k) \tag{1b}$$

with ρ and σ positive scalars.

Therefore, the discrete-time evolution of the j-th cell within the pack can be captured in terms of the state vector of its anode $(\text{x}_j(k) = [\text{SOC}_j(k) \text{CSC}_j(k)]^{\text{T}}$

$$\text{x}_j(k+1) = \text{A}_j \text{x}_j(k) + \text{B}_j \text{I}_j(k), \tag{2}$$

where $\text{I}_j(k)$ is the current applied to the j-th cell, and

$$\text{A}_j = \begin{bmatrix} 1 & 0 \\ 1 - e^{-\frac{g_j}{\chi_j(1-\chi_j)}\text{t}_\text{s}} & e^{-\frac{g_j}{\chi_j(1-\chi_j)}\text{t}_\text{s}} \end{bmatrix}, \quad \text{B}_j = \begin{bmatrix} -\gamma_j \text{t}_\text{s} \\ -\gamma_j \psi_j \end{bmatrix}, \tag{3}$$

$$\psi_j = \text{t}_\text{s} + \frac{e^{-\frac{g_j}{\chi_j(1-\chi_j)}\text{t}_\text{s}} - 1}{\frac{g_j}{\chi_j(1-\chi_j)}} + \frac{1 - e^{-\frac{g_j}{\chi_j(1-\chi_j)}\text{t}_\text{s}}}{\frac{g_j}{\chi_j}}, \tag{4}$$

where g_j, γ_j and χ_j are positive scalars that characterize the diffusion phenomena in the j-th cell, which are ob-

tained with a parameter estimation process using open-loop input current/output voltage profiles. t_s is the sampling time of the system.

Each state equation (2) is complemented by a nonlinear output equation that characterizes the only measured variable in each cell: the output voltage. The voltage is express in terms of the cell electrochemical states as

$$\begin{aligned} \mathrm{V}_j(\mathrm{x}_j(k),\mathrm{I}_j(k)) =& \Delta\mathrm{U}_j(\mathrm{x}_j(k)) + \eta_{j_s}^{+}(\mathrm{x}_j(k),\mathrm{I}_j(k)) \\ & -\eta_{j_s}^{-}(x(k),\mathrm{I}_j(k)) - R_{f_j}\mathrm{I}_j(k), \quad (5) \end{aligned}$$

where $\Delta\mathrm{U}_j(\mathrm{x}_j(k)) = \mathrm{U}_j^{+}(\mathrm{x}_j(k)) - \mathrm{U}_j^{-}(\mathrm{x}_j(k))$ is the difference between the equilibrium potentials, a chemistry-dependent nonlinear function that may be found in the literature according to the battery chemistry. This function is also called the open circuit voltage (OCV). $\eta_{j_s}^{\pm}(\mathrm{x}_j(k),\mathrm{I}_j(k))$ are the surface overpotentials given by the Butler-Volmer equation

$$\eta_{j_s}^{\pm}(\mathrm{x}(k),\mathrm{I}_j(k)) = \frac{R\mathrm{T}_{\mathrm{ref}}}{\alpha F}\sinh^{-1}\left(\frac{\mp\theta_j^{\pm}\mathrm{I}_j(k)}{\sqrt{z_j^{\pm}(k)(1-z_j^{\pm}(k))}}\right), \quad (6)$$

where $z_j^{-}(k) = \mathrm{CSC}_j(k)$, $z_j^{+}(k) = \rho_j\mathrm{SOC}(k) + \sigma_j$, with ρ, σ, α $\theta_j^{\pm}$, and R_{f_j} as positive scalars. F is Faraday constant, and R is the universal gas constant. $\mathrm{T}_{\mathrm{ref}}$ is the reference temperature (298.15 K). $\theta_j^{\pm}$ represents the kinematics of the Li-ion movement in each electrode, whereas R_{f_j} represents the ohmic resistance of the anode (Couto et al., 2016).

2.2 Charging Constraints for Li-ion batteries

The main degradation phenomena that might accelerate the loss of capacity and the growth of resistive film layers in the cell electrodes are; i) the lithium plating in the graphite-based anode, and ii) the solvent oxidation in the lithium-based cathode (Hausbrand et al., 2015; Keil and Jossen, 2016). Each of these degradation phenomena (or side reactions) is triggered when the electrode overpotential reaches certain threshold (Chaturvedi et al., 2010). Thus, constraints must be imposed to avoid that the electrodes overpotentials reach the degradation thresholds (i.e., $\eta_{\mathrm{sr}}{}^{+} > 0$ and $\eta_{\mathrm{sr}}{}^{-} < 0$) such as

$$\eta_{\mathrm{sr}}{}^{+}(k) = \eta_s{}^{+}(\mathrm{x}(k),\mathrm{I}(k)) + \mathrm{U}^{+}(\mathrm{x}(k)) - \mathrm{U}_{\mathrm{sr}}{}^{+} \leq 0, \quad (7)$$

$$\eta_{\mathrm{sr}}{}^{-}(k) = \eta_s{}^{-}(\mathrm{x}(k),\mathrm{I}(k)) + \mathrm{U}^{-}(\mathrm{x}(k)) - \mathrm{U}_{\mathrm{sr}}{}^{-} \geq 0, \quad (8)$$

where $\mathrm{U}_{\mathrm{sr}}^{\pm}$ represent the side reaction equilibrium potentials, that are defined in the literature according to the battery chemistry. In the case of graphite based anodes, the plating is characterized by $\mathrm{U}_{\mathrm{sr}}^{-} = 0V$ (Chaturvedi et al., 2010), and for the lithium-cobalt oxide ($\mathrm{LiCoO_2}$) cathodes the solvent oxidation is characterized by $\mathrm{U}_{\mathrm{sr}}^{+} = 4.3V$ (Tang et al., 2009).

Additionally, one must include the EHM limitations that come from the fact that exists a maximum state of charge and surface concentration that holds the linear relation (1a) between the anode and the cathode. Since in equilibrium both concentrations are equalized, the upper bound is common for both of them

$$\begin{bmatrix}\mathrm{SOC}(k)\\ \mathrm{CSC}(k)\end{bmatrix} \leq \begin{bmatrix}\mathrm{SOC}_{\max}\\ \mathrm{SOC}_{\max}\end{bmatrix} \quad (9)$$

The complement of the intersection of the overpotential constraints (7)-(8) and the upper bound for the concentrations (9) describes the charging admissible region for each cell. Due to the nonlinearities of $\mathrm{U}^{\pm}$ and $\eta_s^{\pm}$ in (6)-(8), the admissible region can be found by mapping relations between the critical surface concentration (CSC) and the charging current, which is characterized as the C-rate, i.e., C-rate= $\frac{\mathrm{Current}}{\mathrm{Capacity}}$). The mapping of CSC-I relations can be obtained by using a full electrochemical model and solving the inequalities (7)-(8) for a given constant charging current to verify the conditions $(\mathrm{CSC}, \mathrm{V})$ at which each constraint is violated.

For the case of cells with graphite-based anodes and LCO cathodes, the admissible region, including constraint (9), is illustrated in Fig. 2, where solvent oxidation (blue), plating (red), and overcharge/EHM limitations (orange) are shown. Thus, the intersection of the areas (white+gray) describes the admissible region for the charge and balance of each cell within the pack.

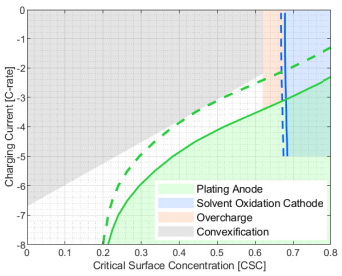

Figure 2. Admissible charging and balancing region.

Fig. 2 shows that constraint (7) is always enclosed by the upper bound (9). However, due to the plating constraint, the admissible region is nonlinear and non-convex, thus not allowing to ensure global optimality and recursive feasibility. To alleviate this problem, a time-invariant convexification can be implemented, transforming the admissible region (7)-(9) into a more conservative time-invariant half-plane defined by the linear constraint

$$\mathrm{I}_j(k) \geq m\mathrm{CSC}_j(k) + b, \quad (10)$$

where the pair $[m, b] = [7.2581, -6.7]$ describes the characteristics the half plane shown in Fig. 2 (gray).

3. PROPOSED SOLUTION

A charge and balance policy should aim at charging each cell as fast as possible, while equalizing SOC imbalances among the cells and accounting for degradation constraints. To perform this in a string Li-ion cells, we consider an active balancing grid that is able to fully shunt the energy of a cell through switches (Fig. 3).To achieve the fast charge and balance, the following elements are needed in the control scheme: i) an extended Kalman filter (EKF) per cell to estimate the non-directly measurable electrochemical states of the cell according to the procedure of (Couto et al., 2016), and ii) a centralized MPC-based policy to manage the charging current and to decide whether the energy is passing or not through a cell.

3.1 Centralized Constrained Control Policy for the fast charge and balance of a string of battery cells

The most widely implemented strategy, that deals with optimal control problems subject to constraints, is the so-called model predictive control (MPC). An MPC policy

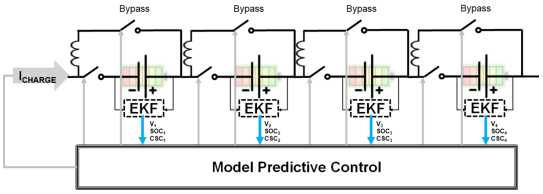

Figure 3. Theoretical balancing grid

computes, at each sampling time, a series of future control actions (a control sequence) by solving an online optimization problem defined by a cost function, and accounting for the process constraints. Due to the receding-horizon approach, only the first component of the control sequence is applied, and the control sequence is re-calculated at the next sampling time.

To describe the fast charge and balance of number ($\mathrm{N_{bat}}$) of serially-connected cells within the MPC framework is necessary to characterize the scenarios where each battery is connected to the balancing grid. As the energy passing through each cell can be shunted through switches (Fig. 3), there exist two scenarios: i) the energy is shunted and the battery is disconnected, and ii) the battery is being charged. To represent both scenarios, an auxiliary binary variable $\lambda_j \in \{0,\,1\} \subset \mathbf{Z}^+$ can be defined per cell as

$$\begin{cases} \lambda_j = 0, & \text{cell by-passed} \\ \lambda_j = 1, & \text{cell being charged.} \end{cases} \tag{11}$$

Therefore, the charge can be suitably regulated by the current of the string (I_{string}) and the connection of the switches of each cell (δ_j)(11). As the objective is to reach a desired state of charge (SOC_{ref}) in the whole string in the shortest time possible, we can define a cost function that does not include any term related to the variations of the charging current ($\Delta \mathrm{I}_{string}$) nor the changes on the charging scenarios ($\Delta\lambda_j$). Thus, the functions along with constraints (9)-(10), and the prediction model (EHM, 1a-6), builds the constrained policy

$$\min_{\mathrm{I}_{string},\Lambda} \sum_{j=1}^{\mathrm{N_{bat}}} \sum_{i=0}^{\mathrm{N}} (\widehat{\mathrm{SOC}_j}(k+i|k) - \mathrm{SOC_{ref}})^2 \tag{12a}$$

s.t.

$$\begin{bmatrix} \widehat{\mathrm{SOC}_j}(k+i+1|k) \\ \widehat{\mathrm{CSC}_j}(k+i+1|k) \end{bmatrix} = \mathrm{A}_j \begin{bmatrix} \widehat{\mathrm{SOC}_j}(k+i|k) \\ \widehat{\mathrm{CSC}_j}(k+i|k) \end{bmatrix} + \mathrm{B}_j \lambda_j(k+i|k) \mathrm{I}_{string}(k+i|k) \tag{12b}$$

$$\begin{bmatrix} \widehat{\mathrm{SOC}_j}(k+i|k) \\ \widehat{\mathrm{CSC}_j}(k+i|k) \end{bmatrix} \leq \begin{bmatrix} \mathrm{SOC_{max}} \\ \mathrm{SOC_{max}} \end{bmatrix} \tag{12c}$$

$$\lambda_j(k+i|k) \mathrm{I}_{string}(k+i|k) \geq m \widehat{\mathrm{CSC}_j}(k+i|k) + b \ . \tag{12d}$$

Note that, although the admissible region for each cell is convex (Fig. 2), the resulting MPC is a nonlinear and non-convex mixed-integer problem due to the product $\lambda_j(k+i|k)\mathrm{I}_{string}(k+i|k)$. This kind of problems is most likely to be NP-hard, i.e. non-solvable in polynomial times, which might be computationally prohibitive and impracticable even for few cells.

A max-min sub-optimal algorithm to solve the mixed-integer nonlinear MPC. As the topology of the string of cells is known, all the possible balancing configurations in the shunting grid can be *a-priori* defined, considering each of them as a subsystem.If each balancing configuration is considered as time-invariant during the prediction horizon, i.e., $\lambda_j(k+1|k) = \cdots = \lambda_j(k+\mathrm{N}|k)$, one can assume that there are no interconnected constraints between the balancing configurations. Accordingly, by duality theory (Boyd and Vandenberghe, 2004), the resulting optimization problem follows the maximization over the current (I_{string}) and the balancing configuration of the string ($\Lambda_{string} = [\lambda_1 \cdots \lambda_{\mathrm{N_{bat}}}]$), while minimizing the charging current of each of the balancing configurations (I_s). This is represented step-by-step in Algorithm 1.

Algorithm 1

A max-min mixed-integer algorithm.

1 DEFINE

$$\mathrm{S} = \begin{bmatrix} 1 & 0 & \cdots & 0 \\ 0 & 1 & \cdots & 0 \\ \vdots & \vdots & \ddots & \vdots \\ 1 & 1 & \cdots & 1 \end{bmatrix},$$

whose rows $\Lambda_s = [\lambda_1 \cdots \lambda_{\mathrm{N_{bat}}}]$ represent all the binary configurations of the balancing grid, i.e. $s \in [1, \mathrm{N_{config}}]$, with $\mathrm{N_{config}} = 2^{\mathrm{N_{bat}}} - 1$) of the string, i.e., $\mathrm{N_{config}} = 2^{\mathrm{N_{bat}}} - 1$

2 MINIMIZE

$$\mathrm{I}_s = \arg\min_{\mathrm{I}} \sum_{j=1}^{\mathrm{N_{bat}}} \sum_{i=0}^{\mathrm{N}} (\widehat{\mathrm{SOC}_j}(k+i|k) - \mathrm{SOC_{ref}})^2$$

s.t.

$$\begin{bmatrix} \widehat{\mathrm{SOC}_j}(k+i+1|k) \\ \widehat{\mathrm{CSC}_j}(k+i+1|k) \end{bmatrix} = \mathrm{A}_j \begin{bmatrix} \widehat{\mathrm{SOC}_j}(k+i|k) \\ \widehat{\mathrm{CSC}_j}(k+i|k) \end{bmatrix} + \mathrm{B}_j \lambda_{s_j} \mathrm{I}(k+i|k)$$

$$\begin{bmatrix} \widehat{\mathrm{SOC}_j}(k+i|k) \\ \widehat{\mathrm{CSC}_j}(k+i|k) \end{bmatrix} \leq \begin{bmatrix} \mathrm{SOC_{max}} \\ \mathrm{SOC_{max}} \end{bmatrix}$$

$$\lambda_{s_j} \mathrm{I}(k+i|k) \geq m \widehat{\mathrm{CSC}_j}(k+i|k) + b$$

$\forall \Lambda_s \in \mathrm{S}$

3 FIND the maximal charging current to be applied to the string (I_{string})

$$\mathrm{I}_{string} = \arg\max_{\mathrm{I}} |\mathrm{I}_s|$$

4 SELECT all the $S_{I string}$ configurations with $\mathrm{I}_s = \mathrm{I}_{string}$
IF $S_{I string} = 1$ APPLY I_{string} and $\Lambda_{S_{I string}}$
OTHERWISE, FIND and APPLY $\Lambda_{applied}$

$$\Lambda_{applied} = \arg\min_{\Lambda} \sum_{j=1}^{\mathrm{N_{bat}}} \sum_{i=0}^{\mathrm{N}} (\widehat{\mathrm{SOC}_j}(k+i|k)\Big|_{\mathrm{I}_{string}} - \mathrm{SOC_{ref}})^2$$

A pulse width modulation (PWM) approach for the shunting switches. Instead of considering the ideal scenario, where each cell is being charged, or disconnected, for the whole k-th interval of time (11), one can consider a pulse-width modulation (PWM) approach to characterize the switches such as in (Pozzi et al., 2019). This PWM approach considers that each cell is being connected or disconnected during a fraction of the k-th interval of time. The fraction of the time interval is described in terms of the duty cycle of the switch ($d_j \in [0,1] \subset \mathbb{R}$) as

$$\begin{cases} \lambda_j = 0 & k < t < k + d_j T_s, \quad \text{cell by-passed} \\ \lambda_j = 1 & k + d_j T_s < t < k+1, \text{cell being charged} \end{cases} \tag{14}$$

By defining the duty cycle for each cell, the binary variables $\lambda_j(k+i|k)$ within the MPC formulation can be replaced by these duty cycles $d_j(k+i|k)$. Thus, the nonlinear mixed-integer problem is transformed into a nonlinear optimization problem. Although less complex and solvable, the resulting nonlinear MPC (due to product $d_j(k+i|k)\mathrm{I}_{string}(k+i|k)$) might be time-consuming in the current battery management systems, whose computational capabilities are not able to solve complex optimal problems.

To reduce the computational burden of the nonlinear optimization, each duty cycle may be seen as the fraction

of charging current of the string passing through a cell ($d_j = \frac{I_j}{I_{string}}$). This assumption allows considering each cell as an independent subsystem, if and only if the duty cycles are assumed as time-invariant during the control horizon (N) of the individual MPC policy (i.e. $d_j(k+1|k) = \cdots = d_j(k+\mathrm{N}|k)$). Although suboptimal due to this assumption, the resulting optimization follows the maximization over the string current (I_{string}), while minimizing the current of each cell (I_j). This two-level optimization is detailed in Algorithm 2.

Algorithm 2
A ratio-based PWM algorithm.

1 MINIMIZE

$$\mathrm{I}_j = \arg\min_{\mathrm{I}_j} \sum_{i=0}^{\mathrm{N}} (\widehat{\mathrm{SOC}_j}(k+i|k) - \mathrm{SOC}_{\mathrm{ref}})^2$$

s.t.

$$\begin{bmatrix} \widehat{\mathrm{SOC}_j}(k+i+1|k) \\ \widehat{\mathrm{CSC}_j}(k+i+1|k) \end{bmatrix} = \mathrm{A}_j \begin{bmatrix} \widehat{\mathrm{SOC}_j}(k+i|k) \\ \widehat{\mathrm{CSC}_j}(k+i|k) \end{bmatrix} + \mathrm{B}_j \mathrm{I}_j(k+i|k)$$

$$\begin{bmatrix} \widehat{\mathrm{SOC}_j}(k+i|k) \\ \widehat{\mathrm{CSC}_j}(k+i|k) \end{bmatrix} \leq \begin{bmatrix} \mathrm{SOC}_{\max} \\ \mathrm{SOC}_{\max} \end{bmatrix}$$

$$\mathrm{I}_j(k+i|k) \geq m\widehat{\mathrm{CSC}_j}(k+i|k) + b$$

$\forall j$-th cell$\in [1\ \mathrm{N}_{\mathrm{bat}}]$

2 FIND the maximal current of the string I_{string}

$$\mathrm{I}_{string} = \arg\max_{\mathrm{I}} |\mathrm{I}_j|$$

3 FIND d_j by dividing each particular current I_j by the current of the string, i.e.,

$$\mathrm{D} = \begin{bmatrix} \frac{\mathrm{I}_1}{\mathrm{I}_{string}} & \frac{\mathrm{I}_2}{\mathrm{I}_{string}} & \cdots & \frac{\mathrm{I}_{\mathrm{N}_{\mathrm{bat}}}}{\mathrm{I}_{string}} \end{bmatrix}$$

4 APPLY I_{string} and D

4. NUMERICAL IMPLEMENTATION

To evaluate each charging and balancing scheme, we consider a serially-connected virtual string of four graphite-LCO (lithium-cobalt oxide) cells of 160mAh. The common EHM parameters, are reported in Table 1. According to

Table 1. Common cell parameters

$\mathrm{SOC}_{\max}$	0.62	[-]	α	5.00×10^{-1}	[-]
χ	7.00×10^{-1}	[-]	γ	5.45×10^{-6}	$[\mathrm{A}^{-1}\mathrm{s}^{-1}]$
θ^+	3.75×10^{-3}	$[\mathrm{A}^{-1}]$	θ^-	2.39×10^{-3}	$[\mathrm{A}^{-1}]$
ρ	7.99×10^{-1}	[-]	σ	1.01	[-]

Zhang et al. (2014), cell parameters as the anode and electrolyte Li-ion diffusion coefficients and the ohmic film resistance may change along the lifespan. Therefore, to consider the main differences between cells, we include variations of $\pm 50\%$ on the EHM parameters (g_j (4) and R_{f_j} (5)) related to these electrochemical changes.

Table 2. Main cell parametric differences

Cell	1	2	3	4
$g\ [s^{-1}]$	2.13×10^{-2}	4.27×10^{-2}	4.27×10^{-2}	6.40×10^{-2}
$R_f[\Omega\cdot\mathrm{m}^2]$	8.47×10^{-4}	8.47×10^{-4}	4.23×10^{-4}	8.47×10^{-4}

To charge and balance the string of cell with these difference, four strategies are considered:

(1) Strategy 0: A centralized MPC technique without balancing (as a benchmark).
(2) Strategy 1: A max-min mixed-integer balancing algorithm (Algorithm 1) assuming ideal switches in the shunting grid with different reconfiguration times.
(3) Strategy 2: A nonlinear MPC-based strategy assuming pulse-width modulation for the shunting switches, following the strategy presented in Pozzi et al. (2019). This strategy does not consider temperature nor aging like Pozzi et al. (2019) does.
(4) Strategy 3: A ratio-based balancing technique (Algorithm 2) assuming pulse-width modulation for the shunting switches.

The strategies are simulated using a high-fidelity simulator based on a full-EChM (Fast DFN, provided by Prof. S. Moura and the eCAL Department of UC Berkeley), considering a sampling time of 1 s, and over a prediction horizon of $\mathrm{N}-0.05\mathrm{cm} = -0.05\mathrm{cm}10$. Strategies 0, 1, and 3 use the multi-parametric optimization toolbox (Herceg et al., 2013) with a *sedumi solver*. As the multi-parametric optimization toolbox (Herceg et al., 2013) does not afford nonlinear problems, the strategy 2 uses *fmincon* with the *sqp* solver. We do not consider the efficiency of the switches, i.e. energy losses, nor the circuitry for the average current during the simulations.

All the cells within the string are initialized at 3.75V and discharged till one of them reaches a minimal voltage of 3.1V, then the charge of the whole string starts. The charge ends when all the cells reach a desired state of charge equivalent to 97.5% of the maximum allowable state of charge, i.e., $\mathrm{SOC}_{\mathrm{ref}} = 0.975\mathrm{SOC}_{\max}$.

4.1 Results and analysis

With respect to a centralized charging policy without balancing awareness (Strategy 0, Table 3), the max-min mixed-integer policy charges all the cells within the pack, ensuring the desired state of charge at the end of the charge (Strategy 1, Table 3). However, the main disadvantage of implementing a mixed-integer algorithm is the computational time required to execute the charge and the balance simultaneously (Comp. Time, Table 3). Due to the high number of configurations allowed in the string ($2^{\mathrm{N}_{\mathrm{bat}}} - 1$), solving a max-min approach can scale up with higher number of cells within the string. This issue can be alleviated by keeping the balancing configuration for longer times than the charging sampling time. As Table 3 shows, the balancing configuration can be held even for a minute (Reconfiguration Time 60s), without any significant impact on the charging time (less than 1 min), when compared to the case where the charge and balance are done simultaneously at each second (Reconfiguration Time 1s). Therefore, this dramatically reduces the number of reconfiguration changes, thus decreasing computational time, which in the case of few reconfigurations (high reconfiguration times) resembles the time required for a centralized policy without balancing awareness.

In the case of a reconfiguration time of 1min (Reconf. Time 60s), one observes how the charge and balance algorithm sequentially charges the cells from the lowest charged (lowest SOC) to highest charged (Fig 4(a)). Although outperforming a policy without balancing-awareness, the connection and disconnection of cells (Fig. 4(b)) generates a high number of voltage relaxations (Fig. 4(c)) that might lead to stress in the battery or to failures in the battery-pack management system (e.g. the switches).

The implementation of a pulse-width modulation approach reduces the number of configurations changes: each cell is disconnected only when it is fully charged (Figs. 5(a)

and 5(b)). Accordingly, voltage relaxations decrease from several to one per cell (Fig. 5(c)). The reduction of cell connections/disconnections allows PWM approach to outperform the mixed-integer approach in terms of charging time. As seen in Table 3, the charging time of the PWM approach (Strategy 2) is almost three times less than the one obtained by using a mixed-integer approach (Strategy 1), regardless the reconfiguration time.

Although the nonlinear PWM approach reduces the charging time, its maximal computational time doubles the sampling time of the system, thus being prohibitive in a real-time implementation. Instead, when implementing the ratio-based algorithm (Strategy 3), the computational time required (both average and maximal, Strategy 3, Table 3) can be significantly reduced while achieving the same performance in terms of charging time as the obtained with the nonlinear policy (see charging time in Table 3).

Although a PWM approach seems to be the best alternative to charge and balance the string of cells, there are yet two open questions regarding its performance. The first is if this performance will hold when coupling the electrochemical model with a thermal model. The second is which is the best approach to charge the string avoiding to accelerate aging: a) charging the string from the lowest charged cell to the highest one (Mixed-Integer approach), or b) charging the whole string and disconnecting the charged cells (PWM approach). According to Ecker et al. (2014), cell degradation is a function of high SOC, thus leaving some cells fully charged till the end of string charge might not be a conservative/safe approach. However, to address this, some life cycle simulations with an aging model should be carried out with each algorithm, which is beyond the scope of this contribution.

REFERENCES

Altaf, F., Egardt, B., and Mårdh, L.J. (2016). Load management of modular battery using model predictive control: Thermal and state-of-charge balancing. *IEEE Transactions on Control Systems Technology*, 25(1), 47–62.

Boyd, S. and Vandenberghe, L. (2004). *Convex optimization*. Cambridge university press.

Cao, J., Schofield, N., and Emadi, A. (2008). Battery balancing methods: A comprehensive review. In *IEEE Vehicle Power and Propulsion Conference*, 1–6. IEEE.

Chaturvedi, N.A., Klein, R., Christensen, J., Ahmed, J., and Kojic, A. (2010). Algorithms for advanced battery-management systems. *IEEE Control Systems*, 30(3), 49–68.

Couto, L.D., Schorsch, J., Nicotra, M.M., and Kinnaert, M. (2016). SOC and SOH estimation for Li-ion batteries based on an equivalent hydraulic model. part i: SOC and surface concentration estimation. In *American Control Conference (ACC)*, 4022–4028. IEEE.

Ecker, M., Nieto, N., Käbitz, S., Schmalstieg, J., Blanke, H., Warnecke, A., and Sauer, D.U. (2014). Calendar and cycle life study of Li(NiMnCo)O2-based 18650 Lithium-Ion batteries. *Journal of Power Sources*, 248, 839–851.

Gallardo-Lozano, J., Romero-Cadaval, E., Milanes-Montero, M.I., and Guerrero-Martinez, M.A. (2014). Battery equalization active methods. *Journal of Power Sources*, 246, 934–949.

Hausbrand, R., Cherkashinin, G., Ehrenberg, H., Gröting, M., Albe, K., Hess, C., and Jaegermann, W. (2015). Fundamental degradation mechanisms of layered oxide Li-ion battery cathode materials: Methodology, insights and novel approaches. *Materials Science and Engineering: B*, 192, 3–25.

Herceg, M., Kvasnica, M., Jones, C., and Morari, M. (2013). Multi-Parametric Toolbox 3.0. In *European Control Conference (ECC)*, 502–510. Zurich, Switzerland.

Hu, X., Perez, H.E., and Moura, S.J. (2015). Battery charge control with an electro-thermal-aging coupling. In *ASME Dynamic Systems and Control Conference*, V001T13A002–V001T13A002. American Society of Mechanical Engineers.

Keil, P. and Jossen, A. (2016). Charging protocols for Lithium-ion batteries and their impact on cycle life: An experimental study with different 18650 high-power cells. *Journal of Energy Storage*, 6, 125–141.

McCurlie, L., Preindl, M., and Emadi, A. (2016). Fast model predictive control for redistributive Lithium-ion battery balancing. *IEEE Transactions on Industrial Electronics*, 64(2), 1350–1357.

Milocco, R.H., Thomas, J.E., and Castro, B. (2014). Generic dynamic model of rechargeable batteries. *Journal of Power Sources*, 246, 609–620.

Perez, H.E., Hu, X., Dey, S., and Moura, S.J. (2017). Optimal charging of Li-ion batteries with coupled electro-thermal-aging dynamics. *IEEE Transactions on Vehicular Technology*, 66(9), 7761–7770.

Pozzi, A., Zambelli, M., Ferrara, A., and Raimondo, D.M. (2019). Balancing-aware charging strategy for series-connected Lithium-ion cells: A nonlinear model predictive control approach. *arXiv preprint arXiv:1902.02122*.

Preindl, M. (2017). A battery balancing auxiliary power module with predictive control for electrified transportation. *IEEE Transactions on Industrial Electronics*, 65(8), 6552–6559.

Preindl, M., Danielson, C., and Borrelli, F. (2013). Performance evaluation of battery balancing hardware. In *European Control Conference (ECC)*, 4065–4070. IEEE.

Quinn, D.D. and Hartley, T.T. (2013). Design of novel charge balancing networks in battery packs. *Journal of Power Sources*, 240, 26–32.

Romagnoli, R., Couto, L.D., Goldar, A., Kinnaert, M., and Garone, E. (2019). A feedback charge strategy for Li-ion battery cells based on reference governor. *Journal of Process Control*.

Samadi, M.F. and Saif, M. (2014). Nonlinear model predictive control for cell balancing in Li-ion battery packs. In *American Control Conference (ACC)*, 2924–2929. IEEE.

Tang, M., Albertus, P., and Newman, J. (2009). Two-dimensional modeling of lithium deposition during cell charging. *Journal of The Electrochemical Society*, 156(5), A390–A399.

Zhang, L., Wang, L., Hinds, G., Lyu, C., Zheng, J., and Li, J. (2014). Multi-objective optimization of lithium-ion battery model using genetic algorithm approach. *Journal of Power Sources*, 270, 367–378.

Table 3. Simulation Results.

Reconfiguration time [s]	Charging time [s]	SOC_{end} [%] Cell 1	Cell 2	Cell 3	Cell 4	Computational Time [s] Average	Max.	Reconfigurations
Strategy 0: MPC central without balance								
-	5.93	39.68	70.83	86.98	97.52	0.073	0.192	-
Strategy 1: Max-min mixed-integer MPC-based algorithm								
1	35.32	97.56	97.79	97.80	97.77	0.830	8.213	1937
15	35.58	97.55	97.99	97.90	97.83	0.127	1.491	132
30	35.63	97.55	97.91	97.84	97.78	0.099	1.450	67
60	36.40	98.79	97.53	99.81	97.75	0.048	0.900	35
120	36.70	97.56	99.86	99.80	97.74	0.041	0.876	18
300	40.93	100.00	99.84	100.00	97.53	0.046	0.694	9
Strategy 2: nonlinear MPC-based policy								
-	12.72	97.53	100.02	100.02	100.02	0.228	2.027	-
Strategy 3: A ratio-based PWM algorithm (Algorithm 2).								
-	12.72	97.53	100.00	100.00	100.00	0.179	0.324	0

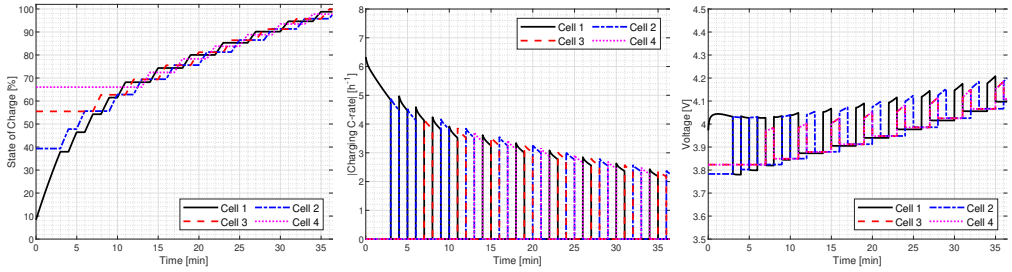

(a) SOC (b) Current (c) Voltage

Figure 4. Performance of strategy 1: Max-min mixed-integer MPC-based algorithm (Algorithm 1, Reconfig. time=60s).

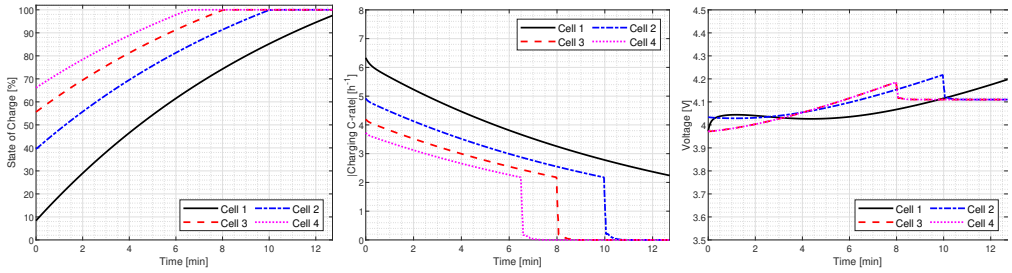

(a) SOC (b) Current (c) Voltage

Figure 5. Performance of strategy 2: nonlinear MPC-based policy.

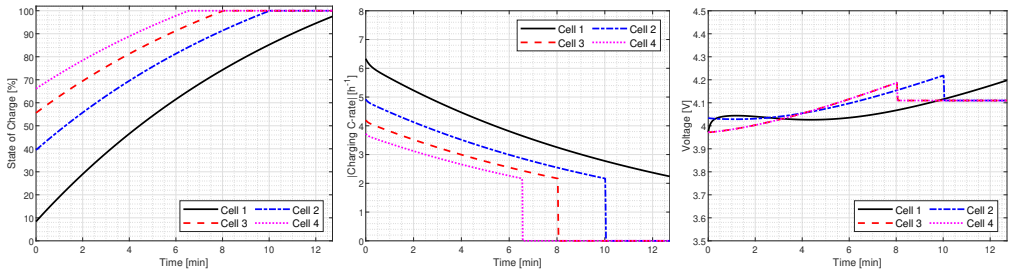

(a) SOC (b) Current (c) Voltage

Figure 6. Performance of strategy 3: A ratio-based algorithm (Algorithm 2).